

**DEVELOPMENT OF MESOPOROUS SILICA NANOPARTICLES
FOR BIOAVAILABILITY ENHANCEMENT OF SOME ANTI HIV
DRUGS**

**A SYNOPSIS
OF THE THESIS TO BE SUBMITTED TO**

**THE MAHARAJA SAYAJIRAO UNIVERSITY OF BARODA
FOR THE AWARD OF DEGREE OF
“DOCTOR OF PHILOSOPHY”
(PHARMACY)**



**Guided
Prof. (Mrs) Sadhana Rajput**

**Submitted by
Mohit Prabhakar Mahajan**

**Pharmacy Department
Faculty of Pharmacy, Kalabhavan Campus
The Maharaja Sayajirao University of Baroda,
Vadodara-390001
September-2017**

SYNOPSIS

Name of the Research Fellow: Mohit P. Mahajan

Project Title: Development of Mesoporous silica nanoparticles for bioavailability enhancement of some anti HIV drugs

Name of Research Guide: Prof. (Mrs.) Sadhana J. Rajput.

Faculty: Faculty of Pharmacy

University: The Maharaja Sayajirao University of Baroda.

1. Introduction

At present, one of the major challenges in the drug development is poor solubility of drug substance which in turn is often responsible for the poor bioavailability of the drugs. As an estimated 40% of all newly developed drugs are poorly soluble or insoluble in water. In addition, up to 50% of orally administered drug compounds suffer from formulation problems related to their low solubility and high lipophilicity.

The solubility and permeability are deciding factors for absorption of the drugs and can be modified through several techniques. The dissolution rate of drugs can be improved by decreasing particle size, decreasing crystallinity, and increasing the surface area. Several studies have been carried out to increase the dissolution rate of drugs by decreasing the particle size by creating nano- and micro particles. ^[1]

Nanoparticles can be used to resolve the problems associated with solubility and bioavailability enhancement. Dissolution of drug is increased due to increase in the surface area of the drug particles from micrometers to the nano-meter size.

Oral ingestion is the most convenient and commonly employed route of drug delivery due to its ease of administration, high patient compliance, cost effective, least sterility constraints, and flexibility in the design of dosage form. However, the major challenge with the design of oral dosage forms lies with their poor bioavailability. The oral bioavailability depends on several factors, including aqueous solubility, drug permeability, dissolution rate, first-pass metabolism, presystemic metabolism, and susceptibility to efflux mechanisms. The most frequent causes of low oral bioavailability are attributed to poor solubility and low permeability. Solubility is one of the important parameters to achieve the desired concentration of drug in the systemic circulation for achieving required pharmacological response. Poorly water soluble drugs often require high and frequent doses in order to reach therapeutic plasma concentrations after oral administration. The poorly water soluble drugs having slow drug absorption leads to inadequate and variable bioavailability and gastrointestinal mucosal toxicity. The poor solubility and low dissolution rate of poorly water soluble drugs in the aqueous gastrointestinal fluids often cause insufficient bioavailability. Especially for class II and class IV drug substances according to the BCS, the bioavailability may be enhanced by increasing the solubility and dissolution rate of the drug in the gastrointestinal fluids. As for BCS class II and IV drugs rate limiting step is drug release from the dosage form and solubility in the gastric fluid and not the absorption, so increasing the solubility in turn increases the bioavailability for BCS class II and class IV drugs. ^[2-6]

One way of increasing the dissolution rate is adsorption of the drug onto a high-surface-area carrier. In this technique, the drug is dissolved in an organic solvent followed by soaking of the solution by a high-surface-area carrier. E.g. Mesoporous silica nanoparticles.^[7]

Mesoporous silica is a form of silica and a recent development in nanotechnology.

According to the nomenclature by IUPAC, Porous materials are classified according to their pore diameter. 1) Micro porous material with a pore size below 2 nm 2) The mesoporous material with a pore size between 2 and 50 nm and 3) The macro porous material with a pore size above 50 nm.

The mesoporous silica nanoparticles are potential drug carriers with following feature:

- A. An ordered pore network:-Very homogenous in size and allow fine control of drug loading and release
- B. High pore volume: - To host require amount of drug substance.
- C. High surface area: - High potential for drug adsorption
- D. A silanol-containing surface: - That can be functionalized to allow better control over drug loading and release.^[8,9]

Initially ordered mesoporous materials were developed for catalysis applications. After that, many researchers recognized their potential applications in many different research areas, such as magnetism, sensors, optical materials, photo catalysis, fuel cells, thermo electrics, and even in the healthcare research area.

In 2001, Maria Vallet-Regi first proposed these ordered mesoporous materials as drug delivery systems. Essentially, pharmaceutical agents were loaded into the mesoporous cavities to be then released as required in the body. The lack of toxicity is necessary for this type of application. An important point within this technology is the host-guest interaction that would take place between the silanol groups located at the surface of the host matrices and the functional groups from the guest molecules. This interaction would have a strong effect on the drug adsorption and release properties of the carrier matrices. Additionally, textural and structural properties have been observed to modulate the adsorption and release characteristics of these ordered mesoporous materials. When dealing with these ordered mesoporous materials for drug delivery, the first and perhaps most important condition is the correct selection of the mesoporous material from all those available depending on the molecule to be hosted. The release of the drug from the mesoporous matrix would take place through diffusion of the drug molecule throughout the pore channels.^[10-15]

These unique features make mesoporous materials excellent candidates for drug-delivery systems. The synthesized mesoporous silica nanoparticles (MSNs) like MCM-41, MCM-48

& SBA-15 are used to enhance the solubility and bioavailability of drug which is loaded in to the pore of mesoporous silica.

1.1 MCM-41:-

In 1992, a research team from Mobil Oil Company synthesized a new family of materials; the so-called M41S that presents ordered pore distributions, with homogeneous sizes ranging between 2 nm -10 nm, including hexagonal-MCM-41. It consists of an amorphous-silicate framework forming hexagonal pores (Fig 1). MCM-41 has high surface areas of up to ~1000 m²/g and large pore volumes. The pores are very uniform causing narrow pore size distributions. The pores are unidirectional and arranged in a honeycomb structure over micrometer length scales. ^[16-19]

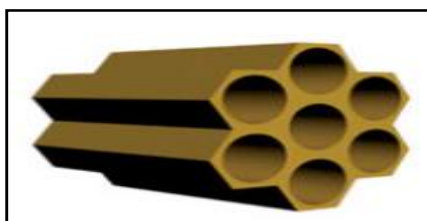


Fig 1 MCM-41 Structure

1.2 SBA-15:-

Santa Barbara Amorphous (SBA-15) which was synthesized for the first time in 1998 by Zhao and co-workers is a kind of mesoporous silica with a hexagonal structure (Fig. 2), large pore size, high surface area, great pore wall thickness, and high thermal stability. ^[20-23]



Fig 2 SBA-15 Structure

1.3 MCM-48:-

MCM-48 has a unique internal structure consisting of enantiomeric pairs of tubular pores that are continuously interwoven and branched to each other, forming a three-dimensional cubic phase (Ia3d) of the pores (Fig 3). This structure has also drawn the attention of researchers for its applicability in drug delivery because the three-dimensional channel topography. ^[24,25]

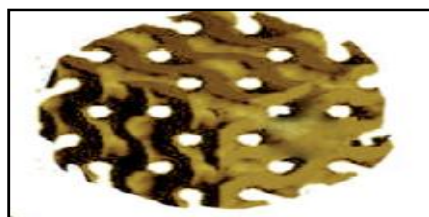


Fig 3 MCM-48 structure

Table 1 Comparison between MSNs

| MCM-41 | MCM-48 | SBA-15 |
|-----------------|---------------------|------------------|
| 2D- Hexagonal | 3D Cubic | 2D- Hexagonal |
| Pore size 2-4.5 | Pore size 1.6-4.0nm | Pore size 5-15nm |
| Thin Pore wall | Thin Pore wall | Thick Pore wall |

2. Selection of Drugs

Acquired immunodeficiency syndrome (AIDS) is a serious disease afflicting several populations of the world. Several classes of the drugs are used in the treatment of AIDS. But most of the newly discovered chemical entities, in spite of high therapeutic activity, have low aqueous solubility and poor bioavailability, leading to poor absorption in the gastrointestinal tracts. For absorption of the drug from the gastrointestinal tracts (GIT), the drug should be present in the solution state in GI fluid, which forms a critical requirement for absorption of poorly water-soluble drugs. Therefore, there is a great interest to develop efficient, reliable, economical, and scalable method to increase the oral bioavailability of poorly water-soluble drugs. HIV protease inhibitors (PIs) are relatively lipophilic molecules and are poorly soluble in water. When dosed orally, insoluble drugs are not efficiently absorbed from the solid state and require specialized formulations to enhance their solubility in the gastrointestinal tract. Consequently, HIV PIs has been associated with high pill counts and large tablets/capsule sizes. Ritonavir (RTV) and lopinavir (LPV) are protease inhibitors (PIs) and practically insoluble in water and could potentially exhibit dissolution rate limited absorption that shows poor bioavailability when administered orally. RTV and LPV is a potent protease inhibitor used for the treatment of HIV infections. Therefore, these two antiretroviral drugs having low solubility and low bioavailability had been selected for the present study considering present need for their new formulations.

2.1 Ritonavir (RTV)

RTV is classified under class II of biopharmaceutical classification system. The class II corresponds to low solubility and high permeability. RTV is a protease inhibitor with activity against Human Immunodeficiency Virus Type 1 (HIV-1). Protease inhibitors block the part of HIV called protease. HIV-1 protease is an enzyme required for the proteolytic cleavage of the viral polyprotein precursors into the individual functional proteins found in infectious HIV-1. RTV binds to the protease active site and inhibits the activity of the enzyme. This inhibition prevents cleavage of the viral polyproteins resulting in the formation of immature non-infectious viral particles. Protease inhibitors are almost always used in combination with at least two other anti-HIV drugs. Modern protease inhibitors require the use of low-dose RTV to boost pharmacokinetics exposure through inhibition of metabolism via the cytochrome P450 3A4 enzyme pathways. IUPAC name of RTV is 1,3-thiazol-5-ylmethyl N-[(2S,3S,5S)-3-hydroxy-5-[[[(2S)-3-methyl-2-[[methyl-[(2-propan-2-yl-1,3-thiazol-4-yl)methyl] carbamoyl] amino]butanoyl]amino]-1,6-diphenylhexan-2-yl]carbamate (Fig. 4). The chemical formula, molecular mass, Log P and melting point of RTV are $C_{37}H_{48}N_6O_5S_2$, 720.948 g/mol, 3.9 and $120^{\circ}C-123^{\circ}C$ respectively. [26-29]

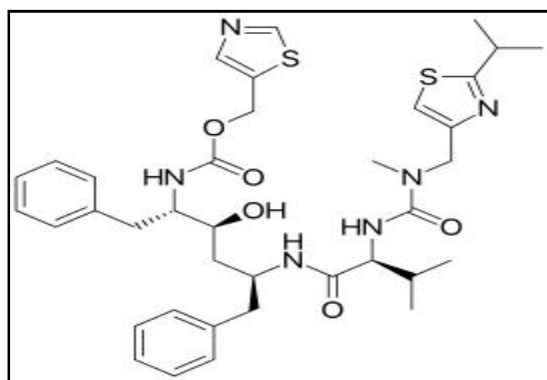


Fig 4. Molecular structure of Ritonavir

2.2 Lopinavir (LPV)

LPV is classified under class IV of biopharmaceutical classification system. The class IV corresponds to low solubility and low permeability. LPV is an antiretroviral of the protease inhibitor class. Inhibiting HIV-1 protease (responsible for protein cleavage), results in selectively inhibiting the cleavage of HIV gag and gag-pol polyproteins, thereby preventing viral maturation. IUPAC name of LPV is (2S)-N-[(2S,4S,5S)-5-[[2-(2,6-dimethylphenoxy)acetyl]amino]-4-hydroxy-1,6-diphenylhexan-2-yl]-3-methyl-2-(2-oxo-1,3-

diazinan-1-yl)butanamide (Fig. 5). The chemical formula, molecular mass, Log P and melting point of LPV are $C_{37}H_{48}N_4O_5$, 628.810 g/mol, 5.94 and 95-98°C respectively. [30,31]

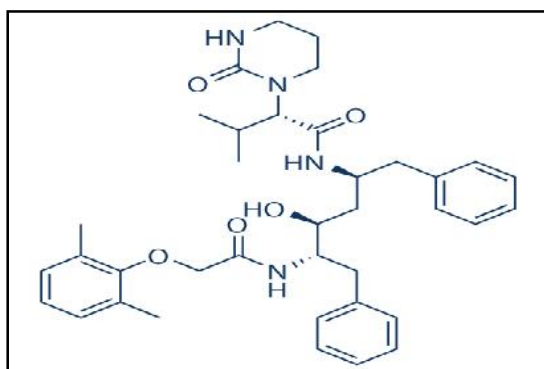


Fig 5. Molecular structure of Lopinavir

3. Aims and Objectives:

The main objective of the study was to develop stable formulations of RTV and LPV by using mesoporous silica nanoparticles for improvement of oral bioavailability by improving its solubility and dissolution properties.

The specific aims of the study were-

- To prepare Mesoporous Silica nanoparticles of MCM-41, MCM-48 and SBA-15.
- To characterize the MSNs by using various Analytical methods. E.g. IR, DSC, XRD, SEM, TEM, N₂ Adsorption-desorption.
- To formulate RTV and LPV drug loaded Mesoporous silica nanoparticles
- To characterize the prepared formulations for its physicochemical properties.
- To prepare tablet formulation of RTV and LPV loaded MSNs and analyze the tablets.
- To carryout *in-vitro* dissolution study of optimized formulation/prepare tablets.
- To evaluate the *in vivo* pharmacokinetics study (Bioavailability study) in Wistar rat from prepared formulations with respect to bulk drug prepare tablets.
- To carryout *in vitro* Cytotoxicity studies of mesoporous silica nanoparticles (MCM-41, MCM-48 and SBA-15) using Caco-2 cell lines (MTT Assay).

4. Experimental

4.1 Materials:

LPV and RTV were obtained as a gift sample from Emcure Pharmaceuticals Pvt. Ltd, Pune, Maharashtra, India. Fumed silica, Tetraethyl-orthosilicate (TEOS), Pluronic P123, Tetraethyl ammonium hydroxide (TMAOH), ammonium hydroxide and Cetyltrimethylammonium bromide (CTAB) were purchased from Sigma- Aldrich, Mumbai, India. Formic acid (HPLC Grade), ethyl acetate and Hydrochloric acid (AR grade) were purchased from Spectrochem Chemicals (Mumbai, India). Polyoxyethylene lauryl ether was purchased from Sigma-Aldrich, Mumbai, India. Acetonitrile and Methanol (HPLC Grade) were purchased from spectro-chemicals, Mumbai, India. Potassium dihydrogen phosphate (AR grade), Sodium dihydrogen phosphate (AR grade) and Sodium hydroxide (AR grade) were purchased from S.D. Fine Chemicals, Mumbai, India Purified HPLC grade water was obtained by filtering double distilled water through nylon filter paper 0.22 μm pore size and 47 mm diameter (Pall Life sciences, Mumbai, India).

4.2 Synthesis of Mesoporous silica nanoparticles (MSNs)

The Synthesis of Mesoporous silica Nanoparticles (MSNs) was carried out using the reported method (MCM-41, MCM-48 & SBA-15) [32-34]. Because the hydrophobic tails of templating surfactants are insoluble in polar solvents and hydrophilic heads of the surfactant in to contact with polar solvents, the surfactants can make self-assembly into micellar liquid crystals at concentrations greater than the “critical micelle concentrations” under certain temperatures. The formed surfactant micelle crystals then serve as the templates for the further formation of inorganic–organic composites around these crystals afterward the addition and subsequent condensation of silica precursors in solution. After the removal of surfactant templates by solvent extraction or calcinations, the mesoporous materials can be obtained. This is the general procedure/mechanism for synthesis of mesoporous silica nanoparticles (Fig 6).

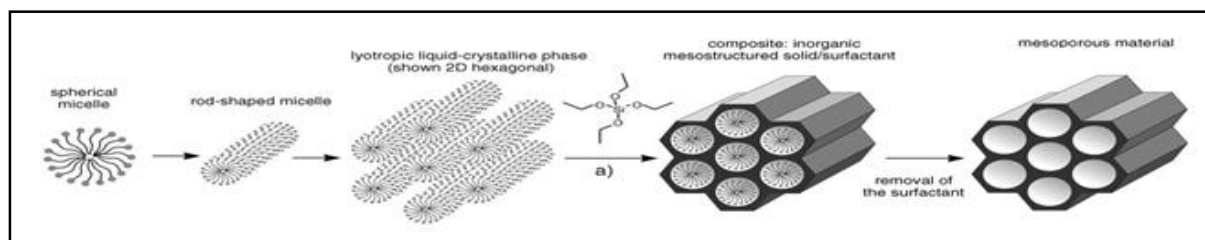


Fig 6 Mechanism for synthesis of mesoporous silica nanoparticles

4.3 Characterization of mesoporous silica nanoparticles (MSNs)

The main characterisation of synthesised MSNs (MCM-41, MCM-48 and SBA-15) was done using techniques like Differential scanning calorimetry (DSC), FTIR, SEM, TEM, low angle Powder-XRD and N₂ Absorption-desorption Technique (BET surface area & porosity measurement). Adsorption analysis gives information about the porosity and surface area of the materials, while Transmission Electron Microscopy (TEM) and scanning electron microscopy (SEM) analysis gives particle size and morphology. Diffraction techniques and TEM supply insight to the degree of structural order, whereas thermal analysis like thermogravimetric Analysis (TGA) and Differential scanning calorimetry (DSC) use for calculating and confirming the drug loading.

4.4 RTV and LPV Loading in Mesoporous silica nanoparticles (MSNs):-

For drug loading different method was used with different solvents. Drug and MSNs in different ratio was also tried for drug loading.

Loading of RTV and LPV individually in MSNs (MCM-41, MCM-48 and SBA-15), various methods and solvents was used. Finally solvent evaporation method was selected and methanol as solvent for drug loading. Best results for loading were obtained using this method.

4.5 Characterization of drug loaded MSNs

After the RTV and LPV drug loading in MSNs (MCM-41, MCM-48 and SBA-15) was completed, the drug loaded MSNs (R-MSNs and L-MSNs) were characterized by Differential scanning calorimetry (DSC), Transmission Electron Microscopy (TEM), N₂ Absorption-desorption Technique, FTIR Technique, and Powder-XRD with the same characterization techniques, to confirm the successful drug loading and results was satisfactory for both drugs.^[35]

4.6 Drug content:

RTV content in the MSNs was determined by dissolving prepared R-MSNs individually (equivalent to 10mg), in methanol. The samples were analyzed spectrophotometrically after appropriate dilution at 240 nm for RTV; from which the drug content was determined.

LPV content in the MSNs was determined by dissolving prepared L-MSNs individually (equivalent to 10mg) in methanol. The samples were analyzed by RP-HPLC, after appropriate dilution at 210 nm for LPV; from which the drug content was determined.

$$\text{Entrapment efficiency} = (\text{weight of drug content in nanoparticles} / \text{weight of feeding drug content}) \times 100$$

4.7. Characterization of RTV Loaded MSNs (R-MSNs) and LPV loaded MSNs (L-MSNs):

4.7.1 Differential Scanning Calorimetry (DSC):

DSC thermograms of bulk drugs RTV and LPV and different types of MSNs (MCM-41, MCM-48 and SBA-15), a physical mixture of drug and MSNs and R-MSNs and L-MSNs were obtained by using DSC 60-A differential scanning calorimeter (Shimadzu, Japan) to find out complete loading of the drug in MSNs and its also find physical state of the drugs. Accurately weighed samples (4-7 mg) were placed in hermetically closed aluminum pans and empty aluminum pan was used as a reference. Heating scans by heat runs for each sample was set from 30 °C to 300 °C at 10 °C min⁻¹ in a nitrogen atmosphere.

4.7.2 Thermogravimetric analysis (TGA)

To determine the amount of RTV and LPV loaded in MSNs, respectively thermogravimetric analysis (TGA) was performed on Shimadzu thermogravimeter TGA-50. TGA thermogram finds the correct range of the drug decomposition. Around 3-10 mg sample was mounted onto the platinum pan, then heated up to 700 °C at a scanning rate of 10 °C/min under a nitrogen gas flow of 50 ml/min. The thermograms were analyzed using TA-60 software.

4.7.3 X-ray Diffraction study:

XRD data for pure drugs LPV and RTV, MSNs (MCM-41, MCM-48 and SBA-15) and final drug loaded MSNs were obtained using X-Pert-PRO X-ray diffractometer, PANalytical (Netherland). Scans were performed in the range of low angle ($1^\circ < 2\theta < 10^\circ$) and at high angle ($3^\circ < 2\theta < 50^\circ$).

4.7.4 Morphology of synthesized MSNs by TEM and SEM:

Morphology of the different synthesized MSNs was studied by Transmission Electron Microscopy (TEM). MSNs and water were mixed and prepare Suspension for analysis .A drop of the suspension was placed on a coated carbon grid and air dried. The grid was then examined immediately under Transmission Electron microscope (TECHNAI-G2 Spirit-Biotwin). The electron micrographs were obtained after magnifications. The physical characteristics of the particles observed by TEM were determined using selected area diffraction (SAD) technique. The measurement conditions were $\lambda = 0.0251 \text{ \AA}$ radiation generated at 120 kV as X-ray source with camera length of 100 cm. The morphology of the MSNs powders was observed under a Scanning Electron Microscope (Hitachi-SU 1510). The samples were mounted directly onto the SEM sample holder using double-sided sticking

carbon tape and images were recorded at the required magnification at the acceleration voltage of 15 kV.

4.7.5 FTIR spectroscopy study:-

The IR spectra of pure drugs (RTV and LPV), MCM-41, MCM-48 and SBA-15 (MSNs), physical mixtures of drug-MSNs and drug loaded MSNs were obtained using a Shimadzu IRAffinity-1, Miracle 10 single reflection ATR mode. Data were collected over a spectral region from 4000 to 650 cm^{-1} with resolution 4 cm^{-1} and 300 scans.

4.7.6 Surface area and pore size study

BET surface area, pore volume and pore diameter of MSNs (MCM-41, MCM-48 and SBA-15) were measured by using Micromeritics ASAP 2010. Prior to characterization, the MSNs samples were degassed under vacuum at high temp for 5Hr, while the drug-loaded MSNs samples were degassed at 40°C for overnight in order to avoid sublimation of drug. The BET specific surface area was calculated by application of the B.E.T. method to the isotherm. The pore volume and pore diameter of both plain MSNs and drug Loaded MSNs were calculated by the nitrogen adsorption-desorption isotherms using the BJH method.

4.8 Formulation of Tablet:-

RTV loaded nanoparticles were formulated in tablet by performing direct compression method. Mixture of different excipients like L-HPC, cross Povidone, MCC, Lactose DCL and Mg. Stearate were utilized and tablets equivalent to 100mg RTV loaded MSNs were punched using single punch tablet machine equipped with punches of 9 mm diameter with flat faces. Tablets were characterized for several parameters like hardness, friability, weight variation, disintegration time etc. as per the official IP methods.

LPV loaded nanoparticles were formulated in tablet by performing direct compression method. Mixture of different excipients like L-HPC, cross Povidone, MCC, Lactose DCL and Mg. Stearate were utilized and tablets equivalent to 200mg LPV loaded MSNs were punched using single punch tablet machine equipped with punches of 12 mm diameter with flat faces. Tablets were characterized for several parameters like hardness, friability, weight variation, disintegration time etc. as per the official IP methods.

5. Analytical Method Development

Ritonavir (RTV)

5.1 UV Spectrophotometric methods for RTV

First standard stock solution (1000 μ g/ml) was prepared by dissolving 10 mg of RTV in 10 ml methanol. Second standard stock solution (10 μ g/ml) was prepared by diluting 0.1 ml of first standard stock solution (1000 μ g/ml) up to 10 ml using Methanol. Then UV-spectrophotometric method of analysis in methanol was developed by first scanning solution of RTV (10 μ g/ml) and determining its λ -max. Further dilutions were made and calibration curve was plotted between 5 and 100 μ g/ml in methanol. The method was validated as per ICH guidelines.

The same process (as described above) was repeated using different diluents (i.e. 0.1N HCl, 1% polyoxyethylene 10 lauryl ether in Acetate Buffer pH-4.5 and 1% polyoxyethylene 10 lauryl ether in water). The methods were validated as per ICH guidelines.

5.2 HPLC Methods for Ritonavir:

Chromatographic studies were performed on Shimadzu (Shimadzu Corporation, Kyoto, Japan) chromatographic system equipped with Shimadzu LC-20AT pump and Shimadzu SPD-20AV absorbance detector. Samples were injected through a Rheodyne 7725 injector valve with fixed loop at 20 μ l.

Chromatographic Conditions

The chromatographic separation was performed using a Kromasil C18 (250 mm \times 4.6 mm i.d., 5 μ m particle size) column. Separation was achieved using a mobile phase consisting of ACN: MeOH: Ammonium Formate Buffer pH 4.5 (40:35:25), pumped at a flow rate of 1.0 ml min⁻¹. The eluent was monitored using a UV detector at a wavelength of 210 nm. The column was maintained at ambient temperature and an injection volume of 20 μ l was used. The mobile phase was vacuum filtered through 0.22 μ m nylon membrane filter followed by degassing in an ultrasonic bath prior to use. Data acquisition and integration were performed using spinchrom software (Spincho Biotech, Vadodara). Injections of 20 μ l were made for each sample concentration and chromatographed under the condition described above. The method was validated as per ICH guidelines.

For detection of RTV from the plasma samples same above method was used. Protein precipitation method was used for the extraction of RTV from plasma samples.

The procedure for the extraction of drug from plasma is as follows:

100 µl of drug spiked plasma sample was piped into a RIA vial and 400 µl of acetonitrile (protein precipitating solvent) was added to it and vortex mixed for 2 min. then samples were centrifuged at 9000 rpm at 4°C for 20 min. From the centrifuged samples approx 400 µl of supernatant was transferred to a sample loading vial and injected into the HPLC system.

5.3 Lopinavir (LPV)

HPLC Methods for LPV

Chromatographic studies were performed on a Shimadzu (Shimadzu Corporation, Kyoto, Japan) chromatographic system equipped with Shimadzu LC-20AT pump and Shimadzu SPD-20AV absorbance detector. Samples were injected through a Rheodyne 7725 injector valve with fixed loop at 20 µl.

Chromatographic Conditions:

The chromatographic separation was performed using a Kromasil C18 (250 mm × 4.6 mm i.d., 5 µm particle size) column. Separation was achieved using a mobile phase consisting of ACN: MeOH: Ammonium Formate Buffer pH 4.5 (40:40:20), pumped at a flow rate of 1.0 ml min⁻¹. The eluent was monitored using a UV detector at a wavelength of 210 nm. The column was maintained at ambient and an injection volume of 20 µl was used. The mobile phase was vacuum filtered through 0.22 µm nylon membrane filter followed by degassing in an ultrasonic bath prior to use. Data acquisition and integration were performed using spinchrom software (Spincho Biotech, Vadodara). Injections of 20 µl were made for each sample concentration and chromatographed under the condition described above. The method was validated as per ICH guidelines.

For detection of LPV from the plasma samples same above method was used. Protein precipitation method was used for the extraction of LPV from plasma samples.

The procedure for extraction of the drug from plasma is as follows:

100 µl of the drug spiked plasma sample was piped into a RIA vial and 400 µl of acetonitrile (protein precipitating solvent) was added to it and vortex mixed for 2 min. then samples were centrifuged at 9000 rpm at 4°C for 20 min. From the centrifuged samples approx 400 µl of supernatant was transferred to a sample loading vial and injected into the HPLC system.

5.4 In vitro release study:

In vitro release studies of pure API, marketed formulation and prepared formulations of RTV were carried out in different dissolution mediums (0.1N HCl, 0.75% polyoxyethylene 10 lauryl ether in Acetate Buffer pH-4.5) using USP dissolution apparatus II (paddle method). And for LPV (0.75% polyoxyethylene 10 lauryl ether in 0.1N HCl, 0.75% polyoxyethylene

10 lauryl ether in Acetate Buffer pH-4.5 and 0.75% polyoxyethylene 10 lauryl ether in phosphate buffer pH-6.8 using USP dissolution apparatus II (paddle method). The experiments were performed on 900mL media at 37°C at a rotation speed of 50 rpm. At preselected time intervals, 5 mL samples were withdrawn, filtered immediately and replaced with 5 mL of fresh dissolution medium. Quantitative determination was performed for RTV and LPV by UV spectrophotometer and RP-HPLC respectively. Graph of percent cumulative drug release vs. time was plotted.

5.5 In vitro cytotoxicity study (MTT Assay)

Cytotoxicity of synthesised MSNs was evaluated for Caco-2 cells using the MTT assay. Caco 2 cells were cultured in 96-well plates for 48 h at a seeding density of 10000 cells/well. All the samples dissolved in DMSO were diluted with DMEM as a culture medium to different concentrations. The final concentration of DMSO was 0.3% (v/v). Experiments were initiated by replacing the culture medium in each well with sample solutions of definite concentration at 37°C in the CO₂ incubator. After 24h h of incubation, the medium was removed and 100 µl of MTT reagent (5mg/ml) in the serum-free medium was added to each well. The plates were then incubated at 37°C for another 24h. At the end of the incubation period, the medium was removed and the intracellular formation was solubilised with 150 µl DMSO and quantified by reading the absorbance at 490nm on a micro-plate multi-detection instrument-680 XR (Bio-Rad Laboratories Ltd, India). Percentage of cell viability was calculated based on the absorbance measured relative to the absorbance of cells exposed to the control and cell free samples.

5.6 In vivo study in Wistar rat

In vivo study of drug loaded MSNs was performed in Wistar rat. The procedure for pharmacokinetic study is as followed:

Bioavailability of RTV and LPV drug loaded MSNs were compared with respective plain drug. Wistar rats were fasted for 12 h prior to the experiment. After oral administration of drug loaded MSNs individually, blood samples were collected through retro-orbital vein into heparinized test tubes at specified time intervals. Blood samples will centrifuged at 5000 rpm for 10 min using a centrifuging machine (Remi centrifuge, Mumbai, India) and plasma samples will be withdrawn and stored at -20°C. The drug content will be determined by developed HPLC method.

6. Results and Discussion

6.1 Synthesis of MSNs:-

Synthesis of different type of mesoporous silica nanoparticles (MSNs) namely MCM-41, MCM48 and SBA-15 was done by different reported method. All synthesized MSNs have different structural and morphological properties. From MCM group we synthesized MCM-41 and MCM-48 with different surface and pore size of nanoparticles, their morphology is also different. MCM-41 had the 2D-hexagonal structure and MCM-48 had 3D cubic structure. One another type of Mesoporous silica nanoparticles was developed; SBA-15 that had 2d hexagonal structure same as MCM-41 but have different pore size and pore structure. Different type of surfactant and silica sources was used with different mole ratio with different temperature and conditions. All MSNs was synthesized successfully.

6.2 Characterization of MSNs

The Characterization of synthesized MSNs (MCM-41, MCM-48 and SBA-15) was done by various techniques like Differential scanning calorimetry (DSC), FTIR, and low angle Powder-XRD, N₂ Adsorption-desorption Technique (BET surface area & porosity measurement). Adsorption analysis gives information about the porosity and surface area of the materials, while Transmission Electron Microscopy (TEM) and scanning electron microscopy (SEM) analysis gives particle size and morphology. All analytical techniques gives very satisfactory results and confirmed successful synthesis of MSNs (MCM-41, MCM-48 and SBA-15)

6.3 Ritonavir and Lopinavir Loading in MSNs

For RTV and LPV loading in MSNs (MCM-41, MCM-48 and SBA-15) respectively, solvent evaporation method was used and methanol was used as loading solvent for both drugs

In preliminary drug loading procedure, fixed amount of RTV and LPV respectively, were dissolved in fixed volume of Methanol and specific amount of MSNs (MCM-41, MCM-48 and SBA-15) was added respectively. The mixture was kept under magnetic stirring at room temperature for 24 h and then removes solvent on rota evaporation at 40°C under high vaccum. The recovered solid was dried for 24 h under vacuum at room temperature and stored. The loading efficiency (LE) within the MSNs was determined indirectly by TGA. Also the drug entrapment efficiency was analyzed by UV-spectrophotometrically/RP-HPLC.

The high drug loading efficiency of MSNs (MCM-41, MCM-48 and SBA-15) was observed for RTV and LPV.

6.4 R-MSNs (R-MCM-41, R-MCM-48 and R-SBA-15) and L-MSNs (L-MCM-41, L-MCM-48 and L-SBA-15)

RTV and LPV drugs were loaded individually in MCM-41, MCM-48 and SBA-15 by solvent evaporation method using methanol as mixing solvent.

The RTV loaded MSNs (R-MSNs) individually called as “R-MCM-41”, “R-MCM-48” and “R-SBA-15” And LPV loaded MSNs (L-MSNs) individually called as “L-MCM-41”, “L-MCM-48” and “L-SBA-15”

6.5 Characterization of R-MSNs and L-MSNs

To confirmed drug loading in MSNs and also confirming no structural changes of MSNs after drug loading, again characterize the R-MSNs and L-MSNs by using the same techniques used above.

6.5.1 Differential Scanning Calorimetry (DSC)

DSC thermogram of RTV, MSNs (MCM-41, MCM-48 and SBA-15), physical mixtures and R-MSNs (R-MCM-41, R-MCM-48 and R-SBA-15) was taken. Pure RTV showed a sharp endothermic peak. Physical mixture exhibited a small endothermic peak for RTV. No obvious peak of the RTV was found in the MSNs after loading, indicating that the drug must be totally entrapped in MSNs and/or present in amorphous state.

DSC thermogram of LPV, MSNs (MCM-41, MCM-48 and SBA-15), physical mixtures and L-MSNs (L-MCM-41, L-MCM-48 and L-SBA-15) was taken. Pure LPV showed a sharp endothermic peak. Physical mixture exhibited a small endothermic peak for RTV. No obvious peak of the LPV was found in the MSNs after loading, indicating that the drug must be totally entrapped in MSNs and/or present in amorphous state.

6.5.2 Thermogravimetric Analysis

TGA thermograms were obtained to evaluate the loading (wt %) of the drug in MSNs (MCM-41, MCM-48 and SBA-15). TGA plots of RTV, LPV and R-MSNs (MCM-41, MCM-48 and SBA-15), L-MSNs (L-MCM-41, L-MCM-48 and L-SBA-15) show their single stepwise weight loss respectively. Thermal behaviour shows the weight loss of RTV and LPV respectively. Based on the % weight loss, the loading capacity of MSNs was determined to be approximately 40%.

6.5.3 Powder-XRD

Powder XRD of RTV, MSNs (MCM-41, MCM-48 and SBA-15) and R-MSNs (R-MCM-41, R-MCM-48 and R-SBA-15) was taken. Pure RTV showed a Sharp and intense crystalline peaks at 2θ of 16.11° , 16.70° , 17.38° , 17.79° , 18.13° , and 21.72° were observed. MCM-41, MCM-48 and SBA-15 showed typical reflections between low angles 2θ , 1° and 8° were observed. P-XRD patterns of R-MSNs (R-MCM-41, R-MCM-48 and R-SBA-15) showed the presence of typical MSNs reflections respectively, but the lack of those relative to the crystalline RTV. This indicates that MSNs kept its structure as it is after loading and no crystalline RTV was detected.

Powder XRD of LPV, MSNs (MCM-41, MCM-48 and SBA-15) and L-MSNs (L-MCM-41, L-MCM-48 and L-SBA-15) was taken. Pure LPV showed a Sharp and intense crystalline peaks at 2θ of 10.61° , 14.84° , 15.63° , 16.53° , 17.43° , and 19.00° were observed. MCM-41, MCM-48 and SBA-15 showed typical reflections between 2° and 8° were observed. P-XRD patterns of L-MSNs (L-MCM-41, L-MCM-48 and L-SBA-15) showed the presence of typical MSNs reflections respectively, but the lack of those relative to the crystalline LPV. This indicates that MSNs kept its structure as it is after loading and no crystalline LPV was detected.

6.5.4 FTIR spectroscopy study

The FT-IR study of pure RTV was exhibit characteristic peaks at $3,480\text{ cm}^{-1}$ (N-H stretching amide group), $2,964\text{ cm}^{-1}$ (hydrogen-bonded acid within the molecule), $1,716\text{ cm}^{-1}$ (ester linkage), $1,658$, $1,606$, and $1,535\text{ cm}^{-1}$ (C-C stretching aromatic carbons). These bands confirm the structure of RTV.

The FT-IR study of pure LPV was exhibit characteristic peaks at $3,375\text{ cm}^{-1}$ (N-H stretching amide group), $3,061\text{ cm}^{-1}$ (OH stretch hydrogen bonded acidic group), $1,660\text{ cm}^{-1}$ (C=O stretching aliphatic aldehydic group), $1,064\text{ cm}^{-1}$ (S=O stretching). These bands confirm the structure of LPV.

FTIR spectrum of MCM-41 exhibit peaks $3,429\text{ cm}^{-1}$ attributable to geminal and associated terminal silanol groups. The stretching vibrations of Si-O-Si and Si-OH can be seen at $1,088\text{ cm}^{-1}$ and 807 cm^{-1} . These bands confirm the structure of MCM-41.

FT-IR spectrum of SBA-15 exhibit peaks at $3,429\text{ cm}^{-1}$ attributable to geminal and associated terminal silanol groups. The stretching vibrations of Si-O-Si and Si-OH can be seen at $1,083\text{ cm}^{-1}$ and 808 cm^{-1} . These bands confirm the structure of SBA-15

The IR spectra of the MCM-48 exhibit peaks at 3433 cm⁻¹ attributable to geminal and associated terminal silanol groups. The stretching vibrations of Si–O–Si and Si–OH can be seen at 1083 cm⁻¹ and 814 cm⁻¹. These bands confirm the structure of MCM-48.

In the physical mixture spectrum of RTV -MCM-41, RTV-MCM-48 and RTV-SBA-15 shows peaks relative to RTV and MCM-41, MCM-48 and SBA-15 (MSNs) respectively, were present as well indicating that the spectrum was the summary of RTV and MCM-41, MCM-48 and SBA-15 (MSNs) spectra that did not display any interactions between the drug and the silicate.

In the physical mixture spectrum of LPV -MCM-41, LPV-MCM-48 and LPV-SBA-15 shows peaks relative to LPV and MCM-41, MCM-48 and SBA-15 (MSNs) respectively, were present as well, indicating that the spectrum was the summary of LPV and MCM-41, MCM-48 and SBA-15 (MSNs) spectra that did not display any interactions between the drug and the silicate.

After RTV loading in the MCM-41, MCM-48 and SBA-15 respectively, spectrum shows a remarkable decrease and slight shifting of the peak. Both changes suggest that in R-MCM-41, R-MCM-48 and R-SBA-15, the majority of the isolated terminal silanol groups interact with RTV.

After LPV loading in the MCM-41, MCM-48 and SBA-15 respectively, spectrum shows a remarkable decrease and slight shifting of the peak. Both changes suggest that in L-MCM-41, L-MCM-48 and L-SBA-15, the majority of the isolated terminal silanol groups interact with LPV.

6.5.5 SEM and TEM

The morphology of MSNs was confirmed by SEM analysis. Well-ordered uniform spherical morphology for MCM-41, SBA-15 and MCM-48 reflected. Regular rope-like 2D hexagonal network formed by MCM-41 and SBA-15 and cylindrical 3D cubic network formed by MCM-48 pore channels were microscopically evaluated from TEM images. TEM images of MCM-41, SBA-15 reveals well-ordered hexagonal arrays with honeycomb pattern and cylindrical cubic pattern for MCM-48-NP.

6.5.6 Surface area and pore size

After RTV and LPV drug loading in MSNs (MCM-41, MCM-48 and SBA-15), BET surface area, pore volume and pore diameter of MSNs were decrease but no changes in isotherm pattern respectively. That mean drug was loaded in pores, present in nanoparticles.

6.5.7 Evaluation of prepared Tablets

Prepared RTV and LPV tablets shows hardness 3.8 to 4.4 kg/cm², disintegration time of 2±0.2 min, friability of below 1% and 98.50-101.65 % drug content values were within the standard limit for all the tablets

6.6 Analytical methods for Ritonavir and Lopinavir:

Ritonavir (RTV):

The max of RTV was found to be 240 nm in methanol, 0.1N HCl (pH-1.2), 0.5% polyoxyethylene 10 lauryl ether in Acetate buffer pH-4.5 and 0.5% polyoxyethylene 10 lauryl ether in water and calibration curves were found to obey Beer's law in the concentration range of 5 to 60 µg/ml with correlation coefficients (R^2) in the range of 0.9990-1.0000.

Calibration curve of HPLC method was plotted in the concentration range of 5-50 µg/ml and showed correlation coefficient (R^2) of 0.999.

Lopinavir (LPV):

For LPV, Calibration curve of HPLC method was plotted in the concentration range of 5-50 µg/ml and showed correlation coefficient (R^2) of 0.9999.

6.7 Dissolution study of Drug Loaded MSNs

Developed RTV and LPV loaded nanoparticles show significant higher release in dissolution media than plain drugs (RTV and LPV).

6.8 Cytotoxicity study

The *in vitro* cytotoxicity studies of MSNs (MCM-41, MCM-48 and SBA-15) in Caco-2 cell lines were performed and reports did not indicate any cellular toxicity.

6.9 In vivo study in Wistar rat

Pharmacokinetic studies in Wistar rat were performed to investigate the improvement in oral bioavailability of RTV and LPV in MSNs respectively and combinely. Plasma drug concentration–time profiles of standard RTV and R-MSNs resulted from the oral administration in Wistar rat, Plasma drug concentration profile of R-MSNs represented significant improvement in drug absorption compared with the standard RTV. For lopinavir, L-MSNs also represented significant improvement in drug absorption compared with the standard LPV. These results indicated that the bioavailability of RTV and LPV in MSNs

were found to be better as compared to attributed to its greater dissolution rate, increased wettability and reduced particle size with increased surface area.

7. Conclusion

The study was undertaken to enhance bioavailability of two poorly water soluble drugs, RTV and LPV. The results of the study demonstrate that the developed mesoporous silica nanoparticles R-MSNs and L-MSNs significantly increase the dissolution and bioavailability of selected drugs in proposed formulations. Hence the proposed formulations of RTV and LPV are allowing a reduction in either the dose or its frequency of administration.

8. Work in progress

Paper and thesis writing is in progress and will be completed soon.

References:-

1. Zaheer A, Maurya N, Mishra K, Santosh, Khan I. Solubility Enhancement Of Poorly Water Soluble Drugs: A Review. *Int J Pharm Tech* 2011; 807-823.
2. Yellela SRK. Pharmaceutical technologies for enhancing oral bioavailability of poorly soluble drugs. *J Bioeq Bioav* 2010; 2(2): 28–36,.
3. Edward KH, Li D. Solubility” in *Drug Like Properties: Concept, Structure, Design and Methods, from ADME to Toxicity Optimization*. Elsevier 2008;56:2008.
4. Vemula VR, Lagishetty V, Lingala S. Solubility enhancement techniques, *Int J Pharma Sci Rev Res* 2010; 5(1):41–51.
5. Sharma D, Soni M, Kumar S, and Gupta GD, Solubility enhancement eminent role in poorly soluble drugs. *Res J Pharm Tech* 2009; 2(2):220–224.
6. Kumar A, Sahoo SK, Padhee K, Kochar PS, Sathapathy A, Pathak N, Review on solubility enhancement techniques for hydrophobic drugs, *Pharm Glob*, 2011; 3(3):1-7.
7. Yadav VB, Yadav AV. Enhancement of Solubility and Dissolution rate of BCS class II Pharmaceuticals by Nanaquious granulation technique. *Int J pharm Res dev* 2008; 1: 1-12.
8. Zhao L, Qin H, Wu r, Zou H. Recent Advances of Mesoporous Materials In Sample Preparation. *J Chromatogr A* 2012; 1228: 193-204.
9. Vallet-Regi M, Balas F, Arcos D. Mesoporous Material for Drug Delivery. *Angew Chem Int Ed* 2007; 46: 7548-7558.
10. Vallet-Regi M, R´amila A, Del Real RP, and P´erez- Pariente J, “A new property of MCM-41: drug delivery system, *Chem Mater* 2001; 13(2): 308–311.
11. Manzano M, Colilla M, Vallet-Regi M, Drug delivery from ordered mesoporous matrices. *Exp Opi Dr Deli* 2009; 6(12):1383–1400.
12. Manzano M, Vallet-Regi M. New developments in ordered mesoporous materials for drug delivery, *J Mat Chem* 2010; 20(27), 5593–5604, 2010.
13. Balas F, Manzano M, Horcajada P, Vallet-Regi M. Confinement and controlled release of bisphosphonates on ordered mesoporous silica-based materials. *J Am Chem Soc* 2006; 128(25):8116–8117.
14. Vallet-Regi M. Ordered mesoporous materials in the context of drug delivery systems and bone tissue engineering. *Chem* 2006; 12(23): 5934–5943.

15. Vallet-Regi M, Mesoporous Silica Nanoparticles: Their Projection in Nanomedicine. *Materials Science* 2012;1-12.
16. Kresge CT, Leonowicz ME, Roth WJ, Vartuli JC, Beck JS. Ordered mesoporous molecular sieves synthesized by a liquid-crystal template mechanism. *Nature* 1992; 359: 710-712.
17. Kresge CT, Leonowicz ME, Roth WJ, Vartuli JC. Synthetic mesoporous crystalline material. U S Patent, 1992; US 5,098,684.
18. Beck JS, Chu CT, Johnson ID, Kresge CT, Leonowicz ME, Roth WJ, Vartuli JC. Method for functionalizing synthetic mesoporous crystalline material. US Patent, 1992; 5,145,816.
19. Beck JS, Vartuli JC, Roth WJ, Leonowicz ME, Kresge CT, Schmitt KD, Chu C, Olson DH, Sheppard EW, McCullen SB, Higgins JB, Schlenker JL. A new family of mesoporous molecular sieves prepared with liquid crystal templates. *J Am Chem Soc* 1992; 114: 10834-10843.
20. Zhao D, Feng J, Huo Q, Melosh N, Fredrickson GH, Chmelka BF, Stucky GD. Triblock copolymer syntheses of mesoporous silica with periodic 50 to 300 angstrom pores. *Science* 1998; 279: 548–552.
21. Zhao D, Huo Q, Feng J, Chmelka BF, Stucky GD. Nonionic Triblock and Star Diblock Copolymer and Oligomeric Surfactant Syntheses of Highly Ordered, Hydrothermally Stable, Mesoporous Silica Structures *J. Am. Chem. Soc.* 1998; 120: 6024–6036.
22. Mohammadi Ziarani G, Lashgari N, Badiei A. *J. Mol. Catal. A: Chem.* 2015; 397: 166–191.
23. Gholamzadeh P, Mohammadi Ziarani G, Lashgari N, Badiei A, Asadiatouei P. *J. Mol. Catal. A: Chem* 2014; 391: 208–222.
24. Kruk M, Jaroniec M. Characterization of High-Quality MCM-48 and SBA-1 Mesoporous Silicas. *Chem. Mater.* 1999; 11: 2568-2572.
25. Schumacher K, Ravikovitch PI, Chesne AD, Neimark AV, Unger KK. Characterization of MCM-48 Materials. *Langmuir* 2000;16: 4648-4654
26. Sinha S, Ali M, Baboota S, Ahuja A, Kumar A, Ali J. Solid Dispersion As An Approach For Bioavailability Enhancement Of Poorly Water-Soluble Drug Ritonavir. *AAPS Pharm Sci Tech* 2010;11(2): 518-528

27. Sarada A, Lohithasu D, Chamundeswari V, Midhun Kumar D, Ramya S. Enhancement of Dissolution Rate of Ritonavir: A Comparative study using various Carriers and Techniques. *Int J Pharma Sci Inv* 2015; 4(8): 44-58
28. Law D, Krill SL, Schmitt EA, Fort JJ, Qiu Y, Wang W, Porter WR. Physicochemical Considerations in the Preparation of Amorphous Ritonavir±Poly(ethylene glycol) 8000 Solid Dispersions. *J Pharma Sci* 2001; 90(8): 1015-1025.
29. Pekamwar SS, Kankudte AD, Kale GK. Formulation And Evaluation Of Solid Dispersion Of Lopinavir By Using Different Techniques. *Int. Res. J. Pharm.* 2015; 6(9): 663-669.
30. Aji Alexa MR, Chackoa AJ, Josea S, Soutob EB. Lopinavir loaded solid lipid nanoparticles (SLN) for intestinal lymphatic targeting. *Eur J Pharma Sci* 2011; 42: 11–18.
31. Goyal G, Vavia PR. Complexation approach for fixed dose tablet formulation of lopinavir and ritonavir: an anomalous relationship between stability constant, dissolution rate and saturation solubility. *J Incl Phenom Macrocycl Chem* 2012; 73:75–85.
32. Vadia N, Rajput S. Study on formulation variables of methotrexate loaded mesoporous MCM-41 nanoparticles for dissolution enhancement. *Eur J Phar Sci* 2012; 45: 8–18.
33. Wang Y, Sun L, Jiang T, Zhang J, Zhang C, Sun C, Deng Y, Sun J, and Wang S. The investigation of MCM-48-type and MCM-41-type mesoporous silica as oral solid dispersion carriers for water insoluble cilostazol. *Drug Dev Ind Pharm.* 2014; 40(6):819-28.
34. Meynen V, Cool P, Vansant EF. Verified Synthesis of Mesoporous Materials. *Micro Meso Matt* 2011; 125: 170-223
35. Qu F, zhu G, Lin H, Zhang W, Sun J, Li S, Qiu S. A Controlled Release of Ibuprofen By Systematically Tailoring the Morphology Of Mesoporous Silica Materials. *J sol stat chem* 2006; 179:2027-2025.